Forschungszentrum Karlsruhe
Technik und Umwelt

Wissenschaftliche Berichte
FZKA 6119

A Lens Model for Applied-B Ion Diodes

I. S. Landman, H. Würz

Institut für Neutronenphysik und Reaktortechnik

Februar 1999

Forschungszentrum Karlsruhe

Technik und Umwelt

Wissenschaftliche Berichte

FZKA 6119

A lens model for applied-B ion diodes

I.S. Landman*, H. Würz

Institut für Neutronenphysik und Reaktortechnik

*permanent address: Troitsk Institute for Innovation and Fusion Research, 142092 Troitsk, Russia

This work was performed in the frame of the Russian German WTZ cooperation agreement RUS-524-96

Forschungszentrum Karlsruhe GmbH, Karlsruhe

1999

Forschungszentrum Karlsruhe GmbH
Postfach 3640, 76021 Karlsruhe

Mitglied der Hermann von Helmholtz-Gemeinschaft
Deutscher Forschungszentren (HGF)

ISSN 0947-8620

Abstract

A one-dimensional model of ion diodes with applied magnetic field was developed based on a perturbation analysis using the Hamilton function for particles and the Vlasov-Maxwell model for the plasma. The Desjarlais 1 dim model was used as initial approximation. First and second order corrections to the 1 dim solution are used for calculating the focal distance of an ion beam.

The gap between the anode and the cathode is considered as a lens that distorts slightly the ion trajectories. The magnetic field generated by the electric current of the diode causes beam focusing. The effect is shown to be of the order of $(V_i/c)^2 << 1$ with V_i the velocity of accelerated ions and c the velocity of light. Distortion of the virtual cathode due to the diamagnetic current of the **E**×**B** electron drift causes an additional focusing of the order of $(\upsilon_D/c)^2 << 1$ with υ_D the characteristic drift velocity.

From the analysis it is concluded that the 1 dim approach is quite adequate for applied-B diodes as long as only the above mentioned focusing mechanisms are most important. Thus a 2 dim numerical simulation may focus mainly on the investigation of small scale turbulent perturbations caused by instabilities in the gap.

Zusammenfassung

Ein Linsenmodell für fremdmagnetisch isolierte Ionendioden

Für fremdmagnetisch isolierte Ionendioden wurde ein 1 dim Modell entwickelt. Teilchen werden mit der relativistischen Hamiltonfunktion, Plasma mit dem Maxwell Vlasov Modell beschrieben. Näherungslösungen erster und zweiter Ordnung werden zur Berechnung der Ionenstrahlfokuslänge benützt. Das 1 dim Desjarlais Modell wird als Ausgangspunkt verwendet.

Der Spalt zwischen der Anode und der Kathode wirkt als Linse welche die Ionenbahnen schwach stört. Das Magnetfeld erzeugt durch den Diodenstrom bewirkt eine Strahlfokusierung proportional zu $(\upsilon_i/c)^2$ « 1 mit υ_i die Ionengeschwindigkeit und c die Lichtgeschwindigkeit. Die Störung der virtuellen Kathode durch den diamagnetischen Strom der Elektronen **ExB** Drift bewirkt einen weiteren Fokussierungseffekt. Dieser ist proportional zu $(\upsilon_D/c)^2$ « 1 mit υ_D der charakteristischen Elektronendriftgeschwindigkeit.

Die durchgeführte Analyse und die erhaltenen Resultate zeigen, daß das 1 dim Modell für fremdmagnetisch isolierte Dioden ausreichend ist, solange die beiden oben genannten Fokussierungseffekte wichtig sind. Eine 2 dim numerische Simulation kann damit auf die Untersuchung turbulenter Störungen im Diodenspalt verursacht durch Instabilitäten beschränkt werden.

Content

1. INTRODUCTION

Essentially two theories are available for describing the operation of a diode principally: the first one of M. Desjarlais [1] and the second one of A.V. Gordeev and A.V. Grechikha [2]. Numerical codes for detailed calculations based mainly on the Particle In Cell simulation (PIC method) of Vlasov-Maxwell equations are also available [3] – [5]. In order to demonstrate the current state of diode investigations a short revue of these publications is given below.

The principal scheme of the diode is shown in Fig. 1 in the Cartesian x- and z-coordinates. In the perpendicular y-direction translation symmetry is assumed. Such plane approximation is rather usual for analytical models of both 'extraction' and 'radial' diode. Magnetic lines of the external field B_{app} belong to the xz-plane. The anode is located at $x = 0$. The cathode of size L is located between the two tips at $z = \pm L/2$. If voltage between the anode and cathode is applied then an ion beam is produced at the anode and a virtual cathode arises between the sharp ends of the tips. The virtual cathode consists of electrons which are produced from the tips of height h by means of field emission at $x = l$.

In Ref. [1] an idealized 1 dim model of the diode is considered. Ions are produced at the anode and are accelerated by the electric field. The electron density in the gap is assumed to be constant. The model explains the behavior of the diode in the frame of a quasi-stationary approach. Current collapse was predicted after the diode voltage reaches the value $\varphi_a = (5/9)A_a$ with A_a the vector potential at the anode. Magnetic self focusing was not modeled. The diamagnetic shift of the virtual cathode towards the anode surface was taken into account. The crossed magnetic and electric fields cause an $\mathbf{E}\times\mathbf{B}$ electron drift. Thus an additional electric current arises along the y-axis. This current changes the applied magnetic field non-homogeneously resulting in a pressure gradient which pushes the virtual cathode to the anode. However distortion of the virtual cathode was not modeled. Therefore diamagnetic focusing of the ion beam was not obtained. The turbulent behavior of the electrons as well as effects of plasma pressure are not considered in this model. This theory claims to describe the diode behavior before the voltage peak.

In Ref. [2] a turbulent distribution of magnetized electrons in the anode-cathode gap is considered in order to explain the unstable behavior of the diode in experiments just after the peak phase. The turbulence is a consequence of the development of the diocotron instability. Using the drift approximation for electrons and assuming a small field emission rate at the virtual cathode it was concluded that for 1 dim geometry the only adiabatic invariant B/n_e should be important for the electron distribution function. Thus the main principal development compared to Ref. [1] is the calculation of the density behavior.

The numerical code KADI2D [3] at FZK is still rather preliminary. A direct simulation of turbulent processes is under development. One of already developed parts of this code is a computational grid generator allowing to map realistic 2 dim geometrical configuration of the gap onto some regular data structure. Another developed part is the solver of the Vlasov-Maxwell problem on the base of the PIC and the Finite Volume (FV) methods.

In Ref. [4] the plasma evolution in the diode with resistive anode plasma layer is considered using a 2 dim PIC code in order to demonstrate the electron sheath collapse. The

ion beam was ignored and the anode plasma resistivity was assumed to be constant. According to first results it seems that the physics of the developing collapse is similar to the interchange instability in the magnetic field. The destabilizing force is caused by the electric field which tries to push rather dense anode plasma through the rare electron sheath.

In Ref. [5] the code QUICKSILVER is described. It was used recently [6] for the numerical simulation of the Particle Beam Fusion Accelerator II. With PBFA II for Li^{+1} beams, pulse duration 20 ns, voltage 10 MV, ion current 0.7 MA, focal power density 1.4 TW/cm^2 an intrinsic beam divergence $\Delta\theta \approx 20$ mrad was obtained. The main goal of these simulation is to find out how to reduce $\Delta\theta$ because for purposes of Inertial Confinement Fusion (ICF) it is necessary to achieve $\Delta\theta \approx 6$ mrad at 30 MV. This code may be considered as most advanced tool available for diode simulations. It is fully vectorized and equipped with many additional programming tools including a pre-processor for grid generation or an output post-processor. Its field solver utilizes both explicit and implicit finite-difference algorithms in Cartesian, cylindrical or spherical coordinate systems. A particle handler advances multiple particle species with three-dimensional relativistic kinematics. At simulations with the computer Cray YMP a three dimensional (r,ϕ,z-coordinates) spatial grid fits to the realistic diode geometry. At this the whole number of 3 dim cells exceeds 10^5, the required number of particles is of 3 10^6. During one simulation the code completes ~ 6 10^4 time steps taking ~ 350 CPU hour. For feed line of the diode a simulation wave guide model was used.

2. RESULTS FROM NUMERICAL SIMULATIONS

Earlier simulations of the diode demonstrated the development of two distinct instabilities: the high frequency diocotron instability and a low frequency ion mode. The diocotron instability is responsible for the fast broadening of the initially narrow electron sheath of the virtual cathode. It arises from wave-electron resonance at the electron drift velocity. It is valid $\omega\tau_i >> 1$ with ω the instability frequency and τ_i the ion gap transit time. The diocotron instability saturates after trapping of electrons by the waves. Then the electrons occupy the whole gap. Ions don't take part in this fast process, i.e. the diocotron instability doesn't induce significant ion beam divergence. In the course of voltage increase the ion current density J_i increases drastically exceeding the Child-Langmuir current J_{CL}. After the ratio J_i/J_{CL} ~ 4 - 8, an abrupt transition to the ion mode instability at much lower frequency ($\omega\tau_i < 1$) occurs which induces significant ion beam divergence.

Calculations of Ref. [6] also detected the diocotron instability early in time followed by a transition to the ion mode later. The characteristic period of the diocotron instability is less than 1 ns, and that of the ion mode is of 2 - 3 ns at $\tau_i \approx 2.5$ ns. The amplitudes of electric field strength of harmonic modes is less than 1 MV/cm. If the ion flux from the anode increases slowly enough, it may cause a delay of the development of the ion mode thus reducing the ion beam divergence.

3. MOTIVATION FOR THIS ANALYSIS

Diode investigations are mainly done by application of large codes. The physics models of the codes are based on the simplest theoretical approach realizing direct numerical solution of most general equations for the fields and matter. Theoretical ideas which allow to clarify effects principally as well as accelerate calculations drastically for the specific considered problem are not included.

Many-fold gain of efficiency may be realized after recognizing parameters intrinsically inherent in the problem (such as the relation $\eta = \lambda/r_e$ of characteristic wave length λ of the instability to the electron gyro-radius r_e). Quite often situations realize where the problem exceeds the technical possibilities of the best computers. Thus making prior theoretical analysis and adequate problem reduction unavoidable. For example, according to a theoretical analysis [7] based on the weak turbulence approach [8] of anomalous electron diffusion across magnetic field in a magneto-electrostatic trap, the parameter η becomes important at $\eta \sim 1$, thus an adequate 3 dim numerical grid must contain more than $(L/r_e)^3 \sim 10^9$ cells for 100 eV electrons which is impossible to be handled by present day machines.

One remarkable feature of the calculational results from Ref. [6] is the rather low level of the perturbation fields in comparison with the quasi-stationary ones (for the electric field strength it was calculated $\delta E/E < 1/5$). Such smallness could be a quite natural assumption for the whole problem because the goal of diode investigations is minimization of the ion beam divergence which may be possible only at low perturbation levels.

Hence for the analysis of applied-B ion diode it is quite reasonable to use methods of perturbation theory. As an initial approximation a quasi-stationary state is assumed. The particle distribution function f_0 and the self-consistent field ψ_0 are reflecting the initial symmetry of the unperturbed system (e.g. independence on the coordinates y and z). In this paper only those small perturbations δf and $\delta\psi$ are considered which are caused by voltage increase. The equations for $f_0 + \delta f$, $\varphi_0 + \delta\psi$ are derived from general Vlasov and Maxwell equations using the Hamilton function of particles.

In chapter 4 general mathematical expressions are given and in chapter 5 a 1 dim model of the diode is considered describing the initial approximation. Principally this 1 dim approach is similar to the Desjarlais model [1]. First and second order corrections are then calculated in order to get the focal distance F. Thus the gap between the anode and cathode is considered as a lens that distorts slightly the ion trajectories. In chapter 6 the influence of a first order additional magnetic field generated by the electric current through the diode is analyzed. This field causes focusing of the ion beam because it bends the ion trajectories. In chapter 7 the focusing effect of the distortion of the virtual cathode is analyzed. This distortion is due to a diamagnetic electron drift current which decreases the magnetic strength near the cathode causing a second order 2 dim change of electric field in the gap. Thus the acceleration of ions changes its direction resulting in focusing.

A relativistic approach seems to be not necessary for the description of an applied B ion diode because ions are evidently non-relativistic particles. As to electrons they lose their kinetic energy in the course of their relatively slow turbulent diffusion from the virtual cathode to the anode through an electric potential drop of several MV thus keeping their characteristic velocity much smaller than the light speed. But due to the lack of evidence a

relativistic description of electrons will be used. For the considered Vlasov-Poisson model based on the Hamilton function of plasma particles the relativistic generalization doesn't lead to additional complexity.

4. GENERAL EQUATIONS

The formulas of this chapter are taken from Ref. [9,10]. The relativistic Hamilton function H_α of an electron (index α = 'e') or ion (α = 'i') is given as:

$$H_\alpha(t,\mathbf{r},\mathbf{p}) = q_\alpha\varphi(t,\mathbf{r}) + \left(m_\alpha^2c^4 + c^2\left(\mathbf{p} - (q_\alpha/c)\mathbf{A}(t,\mathbf{r})\right)^2\right)^{1/2} \tag{1}$$

with charges q_e = -e and q_i = e , masses m_α , the elementary charge e and the velocity of light c. The electromagnetic field is described with the scalar electric potential φ and the vector magnetic potential **A**. Time t, position **r**, canonical momentum **p** are the coordinates of the problem. The field strengths **E** and **B** are expressed as

$$\mathbf{E} = -\frac{1}{c}\frac{\partial\mathbf{A}}{\partial t} - \nabla\varphi, \qquad \mathbf{B} = \nabla\times\mathbf{A} \tag{2}$$

The Maxwell equations for the potentials φ and **A** are given as

$$\frac{\partial\varphi}{\partial t} + c\nabla\mathbf{A} = 0 \quad \text{(the Lorenz gauge)} \tag{3}$$

$$\frac{\partial^2\varphi}{c^2\partial t^2} - \Delta\varphi = 4\pi e(n_i - n_e) \tag{4}$$

$$\frac{\partial^2\mathbf{A}}{c^2\partial t^2} - \Delta\mathbf{A} = \frac{4\pi e}{c}(\mathbf{j}_i - \mathbf{j}_e) \tag{5}$$

Density $n_\alpha(t,\mathbf{r})$ and flux $\mathbf{j}_\alpha(t,\mathbf{r})$ are expressed via the distribution function $f_\alpha(t,\mathbf{r},\mathbf{p})$ and the velocity $\mathbf{v}_\alpha$ of particles:

$$n_\alpha = \int f_\alpha d^3p \tag{6}$$

$$\mathbf{j}_\alpha = \int \mathbf{v}_\alpha f_\alpha d^3p \tag{7}$$

The Vlasov kinetic equation for the function $f_\alpha(t,\mathbf{r},\mathbf{p})$ is given as

$$\frac{\partial f_\alpha}{\partial t} + \{H_\alpha, f_\alpha\} = 0 \tag{8}$$

with {,} the Poisson brackets. Boundary conditions for Eqs. (4), (5) and (8) are given in the course of the further considerations.

The momentum **p** is expressed via the velocity as

$$\mathbf{p} = \gamma_\alpha m_\alpha \mathbf{v}_\alpha + \frac{q_\alpha}{c}\mathbf{A} \tag{9}$$

with the module $\upsilon_\alpha=|\mathbf{v}_\alpha|$[1] and the relativistic factor $\gamma_\alpha = [1-(\upsilon_\alpha/c)^2]^{-1/2}$. Expressing γ_α from Eqs. (1) and (9) as

$$\gamma_\alpha m_\alpha = \frac{H_\alpha - q_\alpha\varphi}{c^2}$$

and then $\mathbf{v}_\alpha$ via **p** as

$$\mathbf{v}_\alpha = \frac{c^2}{H_\alpha - q_\alpha\varphi}\left(\mathbf{p} - \frac{q_\alpha}{c}\mathbf{A}\right)$$

the flux of Eq. (7) is transformed as:

$$\mathbf{j}_\alpha = \int \frac{c^2}{H_\alpha - q_\alpha\varphi}\left(\mathbf{p} - \frac{q_\alpha}{c}\mathbf{A}\right) f_\alpha d^3p \tag{10}$$

5. INITIAL QUASI-STATIONARY APPROACH

5.1. Formulation of the one dimensional problem.

Initially it is assumed that the diode operation is quasi-stationary and with translational symmetry along the y- and z-axes. The position $x = l$ in Fig. 1 corresponds to the undisturbed surface of the virtual cathode. The applied magnetic field is directed along the z-axis and is described by the y-component only: $\mathbf{A}_0 = (0, A_{y0}(x), 0)$. Both electric $\varphi_0(x)$ and magnetic $A_{y0}(x)$ potentials are zero at the virtual cathode and assigned with given values $\varphi_0(0) = \varphi_a > 0$, $A_{y0}(0) = A_a > 0$ at the anode[2].

Then the Hamilton function of Eq. (1) is given as

$$H_{\alpha 0}(x,\mathbf{p}) = \left(m_\alpha^2c^4 + c^2\left(p_x^2 + \left(p_y - \frac{q_\alpha}{c}A_{y0}(x)\right)^2 + p_z^2\right)\right)^{1/2} + q_\alpha\varphi_0(x) \tag{11}$$

Due to the independence of $H_{\alpha 0}$ on t, y and z the Poisson brackets $\{H_{\alpha 0},H_{\alpha 0}\}$, $\{H_{\alpha 0},p_y\}$, $\{H_{\alpha 0},p_z\}$ are equal to zero, thus $H_{\alpha 0}$ and the momentum components p_y, p_z keep constant along

[1] the k-component ($k=x,y,z$) of particle velocity is designated below as $\upsilon_{\alpha k}$.

[2] The index 0 indicates the functions of the initial ('zeroth') approximation.

an unperturbed particle trajectory [9]. Eq. (8) gets stationary showing that the value of the function $f_{\alpha 0}$ is also a trajectory integral:

$$\{H_{\alpha 0}, f_{\alpha 0}\} = 0 \tag{12}$$

A complete integral of Eq. (12) is an arbitrary function $f_{\alpha 0}(H_{\alpha 0}, p_y, p_z)$ of the others integrals.

Ions appear with zero velocity at the anode, pass the gap and disappear at the cathode. Thus their distribution function is determined by the anode emission and is given as

$$f_{i0} = j_{ix1}(0)\delta(H_{i0} - m_i c^2 - e\varphi_a)\delta(p_y - eA_a/c)\delta(p_z) \tag{13}$$

with the Dirac function $\delta(\xi)$[3]. The x-component of the ion flux at the anode $j_{ix1}(0)$ is determined by the anode emission being introduced with the additional index 1 which indicates first order approximation values. If the component j_{ix} would be the value of the initial approximation then in accordance with Eq. (5) it would generate an x-component of magnetic potential A_x that is not taken into account at the initial approximation. In other words it is valid the equality $\mathbf{j}_{i0} = 0$ in the expansion $\mathbf{j}_i = \mathbf{j}_{i0} + \mathbf{j}_{i1} + \ldots$

The x-position of the electron gyrating in the applied magnetic field can be characterized by the momentum component p_y. Neglecting the change of electric potential and the magnetic field strength over the x-projection of the gyration trajectory the x-coordinate of the leading center $x_c(p_y)$ is found from the equation

$$p_y + eA_{y0}(x_c)/c = 0 \tag{14}$$

that follows from the condition that $H_{\alpha 0}$ is constant at $eA_{y0}/\gamma m_e c >> \upsilon_\alpha$.

Electron trajectories are infinite spirals along the z-axis, thus controversially to ions there is no boundary condition determining the electron distribution. Therefore in order to find the physical solution for f_{e0} it is necessary to analyze turbulent perturbations of the system thus turning on a collective mechanism of effective particle collisions via electromagnetic field which form their distribution. Such an analysis is a rather complicate task. It seems that all turbulent models which are developed up to this date cannot be applied for the diode properly. Nevertheless in order to consider a simple model it is assumed now that the collisional effect is realized anyhow and corresponding collisional equilibrium is a local Maxwell distribution at the plane $z = 0$ for each position p_y. The equilibrium distribution is characterized then by unknown functions of local electron density $n_{em}(p_y)$ and electron temperature $T_{em}(p_y)$ at the plane z=0 which will be established in the next chapter. This simplification is useful in order to describe the behavior of collisionless electrons because it provides a physically reasonable electron distribution. Hence at the above mentioned small projection of the gyration radius the expression for the function f_{e0} is defined as

$$f_{e0}(H_{e0}, p_y)|_{z=0} = n_{em}(p_y)C_e \exp\left[-\left(H_{e0} + e\varphi_0(x_c(p_y, 0))\right)/T_{em}(p_y)\right] \tag{15}$$

with the solution $x_c(p_y,0)$ of eq. (14) at the plane $z = 0$ and a normalization factor C_e given as

[3] Such an ion distribution function allows to consider ions on the base of formally less complicated hydrodynamic description. But here a more general distribution function formalism is chosen for both ion and electron plasma components.

$$C_e^{-1} = 4\pi \int_0^\infty \exp\left(-\sqrt{m_e^2 c^4 + c^2 p^2}\,/\,T_{em}(p_y)\right) p^2 dp \tag{16}$$

According to this definition there is no explicit dependence of the function f_{e0} on the momentum component p_z. In order to take into account the dependence of the electron distribution on the coordinate z it is assumed that the Boltzmann distribution function with position dependent p_y at arbitrary planes z = constant is valid:

$$f_{e0}(H_{e0}, p_y, z) = f_{e0}|_{z=0} \exp\left[\left(e/T_{em}(p_y)\right)\left(\varphi_0\left(x_c(p_y, z)\right) - \varphi_0\left(x_c(p_y, 0)\right)\right)\right] \tag{17}$$

with $x_c(p_y,z)$ the solution of eq. (14) for the coordinate z. Keeping in mind the mentioned assumption the explicit designation of the dependence of function f_{e0} on the coordinate z will be omitted in the following.

Eqs (4) and (5) are reduced to the Poisson equations:

$$\frac{d^2\varphi_0}{dx^2} = 4\pi e(n_{e0} - n_{i0}), \qquad \varphi_0(0) = \varphi_a, \quad \varphi_0(l) = 0 \tag{18}$$

$$\frac{d^2 A_{y0}}{dx^2} = \frac{4\pi e}{c} j_{ey0}, \qquad A_{y0}(0) = A_a, \quad A_{y0}(l) = 0 \tag{19}$$

Despite of absence of the flux $\mathbf{j}_{i0}$ in Eq. (19), the density n_{i0} is not zero due to the relatively small velocity of ions. The Eqs. (6) and (7) for the density and the electron flux are given as:

$$n_{\alpha 0} = \int f_{\alpha 0} d^3 p \tag{20}$$

$$j_{ey0} = \int \frac{c^2}{H_{e0} + e\varphi_0}\left(p_y + \frac{e}{c} A_{y0}\right) f_{e0} d^3 p \tag{21}$$

The functions $f_{\alpha 0}$ depend only on the variables $H_{\alpha 0}$, p_y and p_z. Then it is convenient to use the function $H = H_{\alpha 0}$ as independent variable instead of the momentum component p_x. The expression for p_x is obtained from Eq. (11) as:

$$p_x \equiv p_{\alpha x} = \pm\left[\left(H - q_\alpha \varphi_0\right)^2 / c^2 - m_\alpha^2 c^2 - \left(p_y - q_\alpha A_{y0}/c\right)^2 - p_z^2\right]^{1/2}$$

Then Eqs. (20) and (21) are transformed into

$$n_{\alpha 0} = \int f_{\alpha 0}(H, p_y, p_z) \frac{\partial p_{\alpha x}}{\partial H} dH dp_y dp_z = \int f_{\alpha 0} \frac{H - q_\alpha \varphi_0}{c^2 |p_{\alpha x}|} dH dp_y dp_z \tag{22}$$

$$j_{ey0} = \int \left(p_y + \frac{e}{c} A_{y0}\right) f_{e0} \frac{dH dp_y dp_z}{|p_{ex}|}$$

The contribution from the full distribution function corresponding to different signs of $p_{\alpha x}$ are taken into account at the integration.

In accordance with Eqs. (22) and (7) the following expressions for non-relativistic ions are obtained:

$$n_{i0} = j_{ix1}(0)\left[2e(\varphi_a - \varphi_0)/m_i - (e/cm_i)^2\left(A_a - A_{y0}\right)^2\right]^{-1/2} \tag{23}$$

$$j_{ix1} = j_{ix1}(0), \qquad j_{iz1} = 0 \tag{24}$$

$$j_{iy1} = j_{ix1}(0)\frac{e}{cm_i}\left(A_a - A_{y0}\right)\left[2e(\varphi_a - \varphi_0)/m_i - (e/cm_i)^2\left(A_a - A_{y0}\right)^2\right]^{-1/2}$$

Using Eq. (17) and assuming a weak dependence of the functions n_{em} and T_{em} on p_y the following expressions for electrons are obtained:

$$n_{e0} = n_{em}\theta, \qquad \theta = \exp\left[(e/T_{em})\left(\varphi_0\left(x_c\left(p_y, z\right)\right) - \varphi_0\left(x_c\left(p_y, 0\right)\right)\right)\right] \tag{25}$$

$$j_{ex0} = 0, \qquad j_{ez0} = 0$$

The electron current is obtained as

$$-ej_{ey0} = -cen_{e0}\left(d\varphi_0/dx\right)/\left(dA_{y0}/dx\right) \tag{26}$$

5.2. The one dimensional solution.

To demonstrate the characteristic features of the initial approximation the solution of system of Eqs. (18) and (19) with densities and electron flux given by Eqs. (23), (25) and (26) at given constant values of electron temperature T_{em} and density n_{em} is obtained. The exponential factor θ of Eq. (25) introduces an additional unknown dependence of the density n_{e0} on coordinate z. But for the 1 dim problem the solution is obtained only at $z = 0$. Thus the equality $\theta = 1$ is valid. The anode emission is assumed to be given by the Child-Langmuir space charge limited ion current. The ion current limitation reduces the anode electric field drastically. The virtual cathode[4] provides the electron population in the gap. Turbulence creates anomalous electron diffusion across the gap. It is sufficient to have a relatively small electric field strength $E_c = -d\varphi_0(l)/dx$ at the virtual cathode for driving the anomalous current. Thus at both electrodes zero values of the electric field strength is assumed:

[4] The virtual cathode is a surface of magnetic separatrix between two kinds of magnetic field lines. The first ones belong to the gap, they are rather long and the boundary conditions at their ends can be neglected. The second once occupy the space between the ends of the tips and the surface of the real cathode, they are limited by the metal surfaces of the tips.

$$\left(d\varphi_0/dx\right)_{x=0} = 0 \tag{27}$$

$$\left(d\varphi_0/dx\right)_{x=l} = 0 \tag{28}$$

These boundary conditions will be used in order to find the unknown values of the flux component j_{ix1} and the density n_{e0} which is assumed to be homogeneous.

Eq. (27) should be substantiated additionally. The applied magnetic field strength $B_{z0} = dA_{y0}/dx$ is not zero at the anode. If $E_{x0}(x) = - d\varphi_0/dx$ changes weakly in the vicinity of the anode then the ions may be captured by the magnetic field at the anode and couldn't traverse the gap. Therefore it has to be shown that E_{x0} changes fast enough near the anode to allow the zero value of the $E_{x0}(0)$ as an adequate approximation. This evidence is given in the course of the further analysis.

Eq. (28) can be substantiated in the following way. If it is assumed that there is an electron population in the gap then a source for these electrons as well as a mechanism for their delivery should be provided. The source is the virtual cathode. The transport is by a weak turbulence that develops due to the large electric field in the gap. The turbulence creates an anomalous electron diffusion across the gap. The corresponding 'parasitic' electron current to the anode is neglected. The virtual cathode is effectively connected to the emitting tips along the magnetic lines. Therefore it is sufficient to have a relatively small electric field strength E_c=-$d\varphi_0(l)/dx$ at the virtual cathode to drive the anomalous current. A stable dynamical equilibrium realizes: if the strength E_c is becoming too large then the density n_{e0} will increase due to a large anomalous flux thus decreasing E_c in accordance with Eq. (18), and vice versa. Eq. (28) expresses the neglecting of E_c.

The equation for the magnetic field strength B_{z0} follows from Eqs. (19) and (26) as:

$$\frac{B_{z0}^2}{8\pi} = \frac{B_{z0}^2(0)}{8\pi} - e\left(\varphi_a - \varphi_0\right)n_{e0} \tag{29}$$

According to Eq. (29) at small densities n_{e0} the strength B_{z0} is minimal at the cathode and maximal at the anode (diamagnetic effect due to electron drift). If the density is becoming large, the sign of the strength changes somewhere in between the electrodes. In this case the magnetic potential is a non-monotonic function in the gap. Below the density n_{e0} is assumed to be small enough to get a positive right hand side (RHS) in Eq. (29).

It is convenient to use the potential φ_0 as new independent variable. If E_{x0} is written as a function of φ_0 then Eq. (18) is given as

$$\frac{dE_{x0}^2}{d\varphi_0} = 8\pi e\left(n_{e0} - n_{i0}\right) \tag{30}$$

A relation between the variable φ_0 and the coordinate x is given by the expression:

$$x = \int_{\varphi_0}^{\varphi_a} d\varphi_0'/E_{x0}\left(\varphi_0'\right) \tag{31}$$

Using Eqs. (23) and (27) Eq. (30) is transformed into:

$$\frac{E_{x0}^2}{8\pi} = e j_{ix1}(0) \int_{\varphi_0}^{\varphi_a} \frac{d\varphi_0'}{V_{ix}(\varphi_0')} - e(\varphi_a - \varphi_0) n_{e0} \tag{32}$$

with the ion velocity V_{ix} given as

$$V_{ix}(\varphi_0) = \left(\frac{2e(\varphi_a - \varphi_0)}{m_i} - \left(\frac{e}{m_i c} \right)^2 \left(A_a - A_{y0}(\varphi_0) \right)^2 \right)^{1/2}$$

Eqs. (27) and (32) give the relation interpreted as the equation for the flux $j_{ix1}(0)$:

$$\varphi_a n_{e0} = j_{ix1}(0) \int_0^{\varphi_a} d\varphi / V_{ix}(\varphi) \tag{33}$$

The Eq. (29) is transformed into:

$$A_{y0} = A_a - \int_{\varphi_0}^{\varphi_a} \frac{\left(B_{z0}^2(0) - 8\pi e(\varphi_a - \varphi_0') n_{e0} \right)^{1/2}}{E_{x0}(\varphi_0')} d\varphi_0' \tag{34}$$

From Eq. (34) and the condition ($\varphi_0 = 0 \Rightarrow A_{y0} = 0$) the equation for the magnetic strength $B_{z0}(0)$ follows as:

$$A_a = \int_0^{\varphi_a} \frac{\left(B_{z0}^2(0) - 8\pi e(\varphi_a - \varphi) n_{e0} \right)^{1/2}}{E_{x0}(\varphi)} d\varphi \tag{35}$$

From Eq. (31) and the condition $\varphi_0(l) = 0$ a relation interpreted as the equation for the density n_{e0} follows as:

$$l = \int_0^{\varphi_a} d\varphi / E_{x0}(\varphi) \tag{36}$$

To solve the set of Eqs. (32)-(36) a set of dimensionless variables is used which are introduced by the following expressions:

$$\xi = x/l\,, \qquad u = \varphi_0/\varphi_a\,, \qquad w = A_{y0}/A_a\,, \quad \eta = E_{x0}/\sqrt{8\pi n_{e0}\varphi_a} \tag{37}$$

and a set of dimensionless parameters is defined by the expressions:

$$\varepsilon_i = l/r_i\,, \qquad \varepsilon_D = \lambda_D/l\,, \qquad \varepsilon_a = \varphi_a/A_a \tag{38}$$

with $r_i = V_c/\omega_i$ the ion gyro-radius, $V_c = (2e\varphi_a/m_i)^{1/2}$ the x-component of the ion velocity at the cathode, $\omega_i = eA_a/m_icl$ the ion gyro-frequency and $\lambda_D = (\varphi_a/8\pi en_{e0})^{1/2}$ the Debye length. The flux $j_{ix1}(0)$ and the field strengths $E_{x0}(0)$, $B_{z0}(0)$ are made dimensionless according to:

$$\iota = j_{ix1}(0)/n_{e0}V_c\,, \qquad \eta_0 = E_{x0}(0)/\sqrt{8\pi en_{e0}\varphi_a}\,, \qquad b = B_{z0}(0)/\sqrt{8\pi en_{e0}\varphi_a} \tag{39}$$

As a result the whole problem is transformed to a set of five dimensionless equations for the unknown two functions $\eta(u)$, $w(u)$ and the three numbers ι, b, ε_D:

$$\eta^2 = \iota\int_u^1 (1-u')^{-1/2}\left(1-\varepsilon_i^2\left(1-w(u')\right)^2/(1-u')\right)^{-1/2}du' - 1 + u \tag{40}$$

$$w = 1 - \varepsilon_a\int_u^1 \left(b^2 - 1 + u'\right)^{1/2}\eta^{-1}(u')du' \tag{41}$$

$$\iota\int_0^1 \left(1-u-\varepsilon_i^2\left(1-w(u)\right)^2\right)^{-1/2}du = 1 \tag{42}$$

$$\varepsilon_a\int_0^1 \left(b^2-1+u\right)^{1/2}\eta^{-1}(u)du = 1 \tag{43}$$

$$\varepsilon_D\int_0^1 \eta^{-1}(u)du = 1 \tag{44}$$

Eq. (31) is transformed to the dimensionless view:

$$\xi = \varepsilon_D\int_u^1 \eta^{-1}(u')du' \tag{45}$$

A small value is assumed for the parameter ε_i (the case of small width of the gap compared to the ion gyro-radius). Thus at $\varepsilon_i \to 0$ the term containing ε_i in Eq. (40) is neglected. Due to this simplification Eq. (40) becomes

$$\eta = \sqrt[4]{1-u}\left(2\iota - \sqrt{1-u}\right)^{1/2} \tag{46}$$

From Eqs. (46) and (28) the value of the number ι for which the dimensionless electric field strength η gets zero at the virtual cathode $\iota = ½$ follows. Then Eq. (44) turns into the following expression for the parameter ε_D:

$$\varepsilon_D = \left(\int_0^1 \frac{du}{\sqrt[4]{u}\left(1-\sqrt{u}\right)^{1/2}}\right)^{-1} = \frac{1}{\pi} \tag{47}$$

Thus in accordance with Eq. (38) the density n_{e0} is obtained as $n_{e0} = \pi\varphi_a/8el^2$. Expressing the ion electric current density in accordance with Eq. (39) the Child-Langmuir ion current is obtained as

$$ej_{ix1} = \frac{\pi}{8}\sqrt{e/2m_i}\,\frac{\varphi_a^{3/2}}{l^2} \tag{48}$$

Assuming a small value for the parameter ε_a (large applied magnetic field, i.e. the inequality $b >> 1$ is valid). Eq. (43) is solved with first order accuracy of ε_a by the Taylor expansion of the square root under the integral:

$$\varepsilon_a b\int_0^1\left(1-\frac{u}{2b^2}+\ldots\right)\eta^{-1}(1-u)du = 1$$

resulting in the value of number b as: $b\approx 1/\pi\varepsilon_a+(5/16)\pi\varepsilon_a$. Finally using the additional parameter q the behavior of the dimensionless functions u, η, ξ and w is given by the following expressions:

$$u = 1-q^4 \tag{49}$$

$$\eta = q\left(1-q^2\right)^{1/2} \tag{50}$$

$$\xi = (2/\pi)\left(\arcsin q - q\sqrt{1-q^2}\right) \tag{51}$$

$$w = 1-\xi(q)-\tfrac{5}{12}\pi\varepsilon_a^2 q^3\left(1+\tfrac{4}{5}q^2\right)\sqrt{1-q^2} \tag{52}$$

The dependencies of $u(\xi)$, $w(\xi)$ and $\eta(\xi)$ calculated with Eqs. (49) - (52) are shown in Fig.2. For this demonstration the parameter ε_a=5/9 is chosen which is used in chapter 7.3. In the Desjarlais model the current collapse occurs after the voltage reaches the value $\varphi_a = (5/9)A_a$. The thin dotted diagonal on the plot shows the undisturbed dimensionless magnetic potential at $\varepsilon_a = 0$.

In accordance with Eqs. (49) and (51) the dependence of the dimensionless coordinate ξ on the potential at the vicinity of the anode ($q << 1$) is becoming $\xi \approx (5/3\pi)(1\text{-}u)^{3/4}$. Substituting this dependence into Eq. (52) and neglecting the small contribution of the last term there it is obtained $(1\text{-}w)^2 \sim (1\text{-}u)^{3/2}$. Thus in Eq. (40) the term containing the applied magnetic field parameter ε_i vanishes at $u \to 1$ independently on the value of ε_i. This fact gives the evidence that a solution satisfying Eq. (27) exists for arbitrary applied magnetic field. Hence it is not necessary to introduce a non-zero electric field at the anode to avoid the above mentioned magnetic capture of the ions at the anode.

As the parameters ε_i and ε_a may have arbitrary values a numerical calculation is completed in order to demonstrate the dependence of the parameters b, ι and ε_D on ε_a and ε_i. For the calculation the derivatives of Eqs. (40) and (41) are obtained:

$$\frac{d\eta^2}{du} = 1-\iota\left(1-u-\varepsilon_i^2(1-w)^2\right)^{-1/2}, \qquad \eta(0)=\eta(1)=0 \tag{53}$$

$$\frac{dw}{du} = \varepsilon_a \eta^{-1}\left(b^2 - 1 + u\right)^{1/2}, \qquad w(0) = 0, \qquad w(1) = 1 \tag{54}$$

The solution of the system (53), (54) at given values of parameters b and ι near the electrodes is obtained as:

$$u \to 1: \qquad \eta \to \sqrt{2\iota}(1-u)^{1/4}, \qquad w \to 1 - \tfrac{4}{3}\frac{\varepsilon_a b}{\sqrt{2\iota}}(1-u)^{3/4} \tag{55}$$

$$u \to 0: \qquad \eta \to g\sqrt{u}, \quad w \to \frac{2\varepsilon_a\sqrt{b^2-1}}{g}\sqrt{u} \quad \left(g = \left(1 - \iota/\sqrt{1-\varepsilon_i^2}\right)^{1/2}\right) \tag{56}$$

In order to avoid singularities at the boundary points $u = 0$ and $u = 1$ the numerical integration of Eqs. (53), (54) is completed inside of the interval $u_1 < u < u_2$ with the new boundaries u_1 and u_2 located in the gap rather close to the electrodes: $u_1 << 1$, $(1-u_2) << 1$. Eqs. (55) and (56) are used to establish the new boundary conditions at $u = u_1$, $u = u_2$ for Eqs. (53) and (54). The numerical integration is completed from both boundaries u_1 and u_2 to the intermediate point $u = 1/2$ in order to obtain the corresponding values $\eta_\pm = \eta(1/2\pm0)$, $w_\pm = w(1/2\pm0)$. The deviation function $\delta(b,\iota) = (\eta_+ - \eta_-)^2 + (w_+ - w_-)^2$ is used to find the unknown parameters b and ι minimizing the function δ down to $\delta < 10^{-6}$ with the gradient minimization method. The results of the calculation are shown in Fig. 3. The dependence of the parameters ι and ε_D on ε_a and ε_i is rather weak in comparison with the dependence of the parameter b on ε_a.

6. PERTURBATION ANALYSIS FOR MAGNETIC SELF FOCUSING

6.1. The first order approximation equations.

For the extraction type diode it is sufficient to develop a "theory of thin lens" with a small bend of the ion trajectories in the z-direction caused by A_x (the far external focusing). The principal scheme for calculation of the focal distance F is shown in Fig. 4. The solution of the self consistent system of equations is indicated as a loop diagram in this Fig. Because of quasi-stationary operation the time derivatives in the Vlasov and Maxwell equations are omitted in the scheme. Solutions of the Vlasov equation $\{H, f\} = 0$ are determined by the Hamilton function H of particles using appropriate boundary conditions. H is a mathematical expression for the energy via spatial coordinates and canonical momentum of particles. The canonical momentum is contained explicitly in H. The coordinates are contained implicitly via the electric and the magnetic potential.

On first cycle of the diagram the Hamilton function $H = H_0$ with φ_0 and A_{y0} obtained in the previous chapter is used in the Vlasov equation $\{H,f\} = 0$ as it is indicated in the upper left box of Fig. 4. Then (following the arrow) the obtained zeroth order solution of the Vlasov equation $f = f_0$ is used for the calculation of the density and the first order approximation particle flux. Using these results at the RHS of the Maxwell equations first order corrections to the potentials are obtained (the down right box). The corrected potentials are substituted (following the arrow) into the Hamilton function resulting in the first approximation H_1 for $H = H_0 + H_1$ which determines the first order solution $f = f_0 + f_1$ of the Vlasov equation (again the upper left box). In order to obtain next order corrections this cycle is repeated.

If $j_{ix1} \neq 0$ then in accordance with Eq. (5) a x-component of the magnetic potential A_x does exist. After neglecting A_z at the first order approximation from Eq. (3) for the stationary problem follows that A_x is a function of z only. Thus p_z can't be derived as motion integral and the problem is limited principally in the z-direction. Hence ions are accelerated in z-direction. Symmetry with respect to the plane $z = 0$ is assumed. The acceleration of ions causes magnetic self-focusing. The scheme of the magnetic self focusing for an extraction diode is shown in Fig. 5. The magnetic strength component $B_y = \partial A_x/\partial z$ is assumed to exist only in the gap because of a compensation of the ion beam current by electron current outside of the gap. Due to the current compensation the ions are propagating straightforward after passing the virtual cathode and then arrive at the focal point F. The small bend implies the introduction of a small parameter describing contributions from A_x. The value of this parameter is obtained at the end of this chapter. The perturbation source is the x-component of the ion flux j_{ix1}. Therefore in accordance with Eq. (5) the component A_x is the first order perturbation. The non-zero ion flux in the z-direction causes the z-component of magnetic potential A_z to be non-zero[5]. But A_z appears only as a second order perturbation because according to Eq. (24) the equality $j_{iz1} = 0$ is valid. The slow change of the ion beam parameters along the z-direction allows to assume that the derivatives of the initial approximation functions on coordinate z are negligibly small compared to those on coordinate x. It is necessary to carry out the first order approximation analysis only for ions because for electrons the assumption about the Boltzmann distribution as discussed in chapter 5.1 is sufficient.

For a first order correction H_{i1} of the ion Hamilton function it is obtained from Eq. (1):

$$H_{i1} = -\frac{c^2}{H - e\varphi_0} p_{ix} \frac{e}{c} A_{x1} \tag{57}$$

In order to demonstrate characteristic features of the first order approximation the small $A_{y1}$is neglected in Eq. (57). As to a correction of H_{i1} by φ_1 it is shown below that the equality $\varphi_1 = 0$ is valid.

The stationary Vlasov equation of the first order approximation is obtained from Eq. (8) as

$$\{H, f_{i1}\} + \{H_{i1}, f_{i0}\} = 0 \tag{58}$$

The Maxwell equations (3)-(5) write as:

$$\frac{\partial A_{x1}}{\partial x} = 0 \tag{59}$$

$$\frac{\partial^2 A_{x1}}{\partial z^2} = -\frac{4\pi e}{c} j_{ix1}, \qquad A_{x1}|_{z=0} = 0, \qquad dA_{x1}/dz|_{z=0} = 0 \tag{60}$$

[5] In principle the z-component of the ion flux could be compensated locally by the electron flux. But as long as the Boltzmann distribution is valid the electrons are allowed to move only along the surfaces of constant position p_y, i.e. their flux x-component is absent: j_{ex1}=0. From the continuity equation div$\mathbf{j}_e$ = 0 then follows that at first order approximation the electron flux z-component is also zero: $j_{ez1} = 0$.

6.2. The first order solution.

From Eqs. (59) and (60) an expression for the component A_{x1} follows as:

$$A_{x1}(z) = -\frac{2\pi e}{c} j_{ix1}(0) z^2$$

thus from Eq. (57) it follows:

$$H_{i1} = \frac{2\pi e^2 j_{ix1}(0) z^2 p_{ix}}{H - e\varphi_0} \tag{61}$$

and from Eq. (58)

$$\frac{d}{dt}\left(f_{i1} - H_{i1} \frac{\partial f_{i0}}{\partial H} \right) = \frac{\partial f_{i0}}{\partial p_z} \frac{\partial H_{i1}}{\partial z} \tag{62}$$

with the symbol d/dt designating the time derivative along an unperturbed trajectory. From Eq. (62) the expression for the function f_{i1} is obtained as:

$$f_{i1} = \frac{\partial f_{i0}}{\partial H}\left(H_{i1} - H_{i1}|_{t=0} \right) + \frac{\partial f_{i0}}{\partial p_z} \int_0 \frac{\partial H_{i1}}{\partial z}(t')dt' \tag{63}$$

In Eq. (63) the time integration is carried out along an unperturbed trajectory, the time t plays the role of the coordinate along the trajectory. At the initial time moment $t = 0$ the perturbation of the distribution function is zero: $f_{i1}|_{t=0} = 0$. For ions $t = 0$ is the start from the anode with zero value of the x-component of the momentum: $p_{ix}|_{x=0} = 0$. From Eq. (61) the condition $H_{i1}|_{t=0} = 0$ follows. At the zeroth approximation there is no acceleration towards the z-axis. Thus the coordinate z is constant while the integration along the unperturbed ion trajectory and the z-component p_{iz} of the momentum is equal to zero. Neglecting in Eq. (61) a weak dependence of the function φ_0 on coordinate z, replacing the variable under the integral in Eq. (63) by the substitution $dt = dx/v_{ix}$ and using the non-relativistic relation $p_{ix} = m_i v_{ix}$ the resulting expression for function f_{i1} is obtained from Eq. (63) as:

$$f_{i1} = \frac{2\pi e^2 j_{ix1}(0) z}{H - e\varphi_0}\left(z p_{ix} \frac{\partial f_{i0}}{\partial H} + 2 m_i x \frac{\partial f_{i0}}{\partial p_z} \right) \tag{64}$$

Eqs. (6) and (10) are transformed to corrections for the ion density and the z-component of the ion flux:

$$n_{i1} = \int f_{i1} \frac{H - e\varphi_0}{c^2 |p_{ix}|} dH dp_y dp_z \tag{65}$$

$$j_{iz2} = \int\left(f_{i1} - f_{i0}\frac{H_{i1}}{H - e\varphi_0}\right) p_z \frac{dH dp_y dp_z}{|p_{ix}|}. \tag{66}$$

Similarly to the ion flux of the first order approximation given by Eq. (66) the ion flux of the second order approximation is generated by functions of the lower approximation.

Direct calculation of Eq. (65) results in the equality $n_{i1} = 0$. The Boltzmann electron density can be disturbed only by the potential perturbation φ_1 but according to Eq. (4) φ_1 can be non-zero only due to n_{i1}. Hence the zero value of the potential perturbation $\varphi_1 = 0$ is confirmed.

The expression for the z-component j_{iz2} after some calculations is obtained as:

$$j_{iz2} = -\frac{4\pi e^2 xz}{c^2} j_{ix1}^2(0)\left[2m_i e(\varphi_a - \varphi_0) - (e/c)^2\left(A_a - A_{y0}\right)^2\right]^{-1/2}$$

For an estimation of the focus distance F it is assumed that after reaching the cathode the ions which have initially some coordinate z are going further straightforward. In this case F is given by the expression:

$$F = z\,\mathrm{ctg}\,\beta \tag{67}$$

with β the angle under which the ions are crossing the plane $z = 0$. β is determined by the ratio of z- to the x-component of the ion flux at the cathode plane $x = l$. Using Eq. (39) with dimensionless flux $\iota = 1/2$ and Eq. (38) for substitution of the parameter ε_D into the flux relation as well as Eq. (47) for ε_D the tangent of β is obtained as

$$\mathrm{tg}\,\beta = \left|j_{iz2}/j_{ix1}\right|_{x=l} = \frac{\pi^2}{8}\left(\frac{V_c}{c}\right)^2 \frac{z}{l} \tag{68}$$

From Eqs. (67) and (68) the resulting expression for F follows as:

$$F = l\frac{8}{\pi^2}\left(\frac{c}{V_c}\right)^2 \tag{69}$$

According to Eq. (69) the inequality $F >> l$ is valid at non-relativistic ion velocities. Hence as long as the perturbation parameter $(V_i/c)^2$ is small the validity of the perturbation analysis for the effect of the magnetic self-focusing is confirmed.

7. DIAMAGNETIC FOCUSING

Another mechanism for ion focusing concerns the mobility of the virtual cathode. The electric and the magnetic potentials are constant at the surface of the virtual cathode. It is assumed that the surface is fixed at the points $(x,z) = (l,\pm L/2)$ of the tip ends. The real cathode

is the surface of constant potentials. In chapter 5.2 it was shown that the magnetic field strength at the virtual cathode decreases due to the electron drift current. But there are no electric currents in the region of constant electric potential $\varphi = 0$ between the virtual and the real cathode (this region is called the cathode region). Thus the virtual cathode surface gets distorted. Its middle part shifts towards the anode in order to keep the momentum equilibrium but the ends are assumed to be fixed. The distortion of the surface results in perturbation of the electric field in the gap and consequently in bending of the ion trajectories. The distorted surfaces A_y = constant inside of the gap are shown in Fig. 6.

To describe small perturbations a sinusoidal function is used in the surface equation

$$\sigma(x,z) = x - l - a_1 \cos(\pi z/L) = 0 \tag{70}$$

with a_1 the amplitude of the first order perturbation. Hence the space between the anode and the real cathode is divided into two regions - the gap and the cathode region - which interact via the surface $\sigma = 0$. Due to the fact that the magnetic field of the current through the diode is neglected, the magnetic field in both regions is described by the y-component of the magnetic potential A_y. The interaction between the two regions is described by the momentum balance at the separating surface. It is assumed that there is no change of the plasma pressure at $\sigma = 0$. The electric field strength is neglected there. Thus the balance equation is reduced to the continuity of the magnetic field pressure across the surface:

$$\left(B^2/8\pi\right)_{\sigma\to-0} = \left(B^2/8\pi\right)_{\sigma\to+0} \tag{71}$$

The magnetic strength at both sides of the surface $\sigma = 0$ is obtained below.

7.1. Magnetic field in the cathode region

The magnetic field is described by the y-component of magnetic potential A_y. At $\sigma > 0$ according to Eq. (5) in the cathode region the Laplace equation is valid:

$$\frac{\partial^2 A_y}{\partial x^2} + \frac{\partial^2 A_y}{\partial z^2} = 0 \tag{72}$$

The boundary conditions for Eq. (72) at the virtual and the real cathode are given as

$$\mathbf{Bn} = 0 \text{ at } \sigma = 0 \text{ and at } x = l + h \tag{73}$$

with $\mathbf{n}=(\partial\sigma/\partial x,0,\partial\sigma/\partial z)$ the normal vector to the surface and $\mathbf{B}=(-\partial A_y/\partial z,0,\partial A_y/\partial x)$. According to Eq. (73) the magnetic potential is constant: $A_y|_{x=l+h} = - A_a h/l$ at the real cathode. At $\sigma = 0$ Eq. (73) expresses the constant value of magnetic potential, too: $A_y = 0$. This condition is conveniently shifted from the perturbed virtual cathode to the plane $x = l$ using the linear Taylor expansion:

$$A_y\left(l + a_1 \cos(\pi z/L), z\right) \approx A_y(l,z) + \left(\partial A_y/\partial x\right)_{x=l} a_1 \cos(\pi z/L) = 0$$

The solution of Eq. (72) is given in first order approximation as

$$A_y = -\frac{A_a}{l}\left(x - l - a(x)\cos(\pi z/L)\right) \tag{74}$$

To satisfy Eq. (73) for small amplitudes a the conditions $a(l)=a_1$, $a(l+h)=0$ are established. Substituting Eq. (74) into Eq. (72) and neglecting small terms a boundary problem for the amplitude $a(x)$ is defined as:

$$\frac{d^2a}{dx^2} - (\pi/L)^2 a = 0, \quad a(l) = a_1, \qquad a(l+h) = 0 \tag{75}$$

The solution of Eq. (75) is obtained as

$$a = a_1 \,\mathrm{sh}(\pi(l + h - x)/L)/\mathrm{sh}(\pi h/L)$$

The magnetic pressure at $\sigma = 0$ from the side of the cathode region is obtained as:

$$\left(B^2/8\pi\right)_{\sigma\to+0} = \frac{A_a^2}{8\pi l^2}\left(1 + 2\pi\frac{a_1}{L}\,\mathrm{cth}(\pi h/L)\cos(\pi z/L)\right) \tag{76}$$

7.2. Magnetic field in the gap

The source of perturbations is the electric potential φ_a applied to the gap because if the equality $\varphi_a = 0$ is valid then there is an unperturbed vacuum magnetic field only in the diode. Therefore φ_a is considered as a small perturbation. In order to use the results of chapter 5.2 small values of the dimensionless parameters ε_i and ε_a are assumed which are defined by Eq. (38). For a small electric potential it is sufficient to use Eqs. (49), (50) and (51) independently from z. But for large magnetic potentials the initial solution has to include the dependence on z thus requiring second order perturbation terms. The magnetic potential in the gap is given as

$$A_y = A_a\left(w|_{\varepsilon_a=0} + \left(w - w|_{\varepsilon_a=0} + l^{-1}a(x)\right)\cos(\pi z/L)\right) \tag{77}$$

with the zero approximation function w given by Eq. (52). Substitution of Eq. (77) into Eq. (5) and separating the terms which are proportional to the factor $\cos(\pi z/L)$ gives an equation for the unknown function $a(x)$:

$$\frac{d^2a}{dx^2} - (\pi/L)^2 a = 0, \quad a(0) = 0, \qquad a(l) = a_1 \tag{78}$$

The non-zero boundary condition at the point $x = l$ in Eq. (78) is obtained as a result of a small shift of the condition from the point $\sigma = 0$ using the Taylor expansion for function A_y:

$$A_y|_{\sigma=0} \approx A_y|_{x=l} + \left(\partial A_{y0}/\partial x\right)|_{x=l}\, a_1 \cos(\pi z/L) = 0 \tag{79}$$

The solution of Eq. (78) is obtained as

$$a = a_1 \,\mathrm{sh}(\pi x/L)/\mathrm{sh}(\pi l/L) \tag{80}$$

The z-component of the magnetic field strength is given by the expression:

$$B_z = \frac{\partial A_y}{\partial x} = \frac{A_a}{l}\left(\frac{dw}{d\xi} + \frac{da}{dx}\cos(\pi z/L)\right)$$

This component is sufficient for a calculation of the magnetic pressure at the boundary $\sigma = 0$ from the side of the gap. According to Eqs. (52) and (80) the magnetic pressure at $\sigma = 0$ calculated from the side of the gap is obtained as:

$$\left(B^2/8\pi\right)_{\sigma\to-0} = \frac{A_a^2}{8\pi l^2}\left(1 + \tfrac{5}{6}\pi\varepsilon_a^2\chi|_{q\to1} - 2\pi\frac{a_1}{L}\,\mathrm{cth}(\pi l/L)\cos(\pi z/L)\right) \tag{81}$$

with the function χ given as

$$\chi = \left(d\xi/dq\right)^{-1}\frac{d}{dq}\left(q^3\left(1 + \tfrac{4}{5}q^2\right)\sqrt{1-q^2}\right)$$

It is obtained $\chi|_{q\to1} = -9\pi/20$.

In the cathode region small perturbations are maximal at the symmetry plane $z = 0$ and vanish at the ends of the electrodes $z = \pm L$. Because the electric potential is applied at every coordinate z, the perturbation doesn't vanish at the planes $z = \pm L$ from the side of the gap. Thus the boundary condition (71) should take into account some additional forces at the ends even for small perturbations. It seems that for the solution of the problem of the focal distance it is not necessary to analyze such effects, hence the end effect at $z << L$ is neglected[6]. As a result the amplitude a_1 is obtained from Eq. (78) as

$$a_1 = -\tfrac{3}{16}\pi L\varepsilon_a^2\left(\mathrm{cth}(\pi l/L) + \mathrm{cth}(\pi h/L)\right)^{-1} \tag{82}$$

7.3 Perturbed motion of ions and the focal distance *F*

In order to find the focal distance F the z-component of the ion flux j_{iz2} is calculated on the base of Eq. (66) in a similar way as described in chapter 6.2. The ion distribution function f_{i1} is given by Eq. (63) with $H_{i1}|_{t=0}=0$.The first approximation correction H_{i1} for the ion Hamilton function Eq. (1) is obtained as

$$H_{i1} = -\left(p_y - m_i\omega_{Li}a\right)\omega_{Li}a\cos(\pi z/L) + e\varphi \tag{83}$$

Estimating values of the functions a, φ and p_y as $a \sim a_1$, $\varphi \sim \varphi_a$ and $p_y \sim m_i V_c$ the magnetic term of the RHS of Eq. (83) is found to be negligibly small at the conditions $l \sim h \sim L$: $p_y\omega_{Li}a/e\varphi_a \sim \varepsilon_i(\varepsilon_a)^2 << 1$. Thus ions are influenced mainly by the electric term $e\varphi$. Up to now

[6] This neglection is a temporary assumption because up to now there is no idea how to take this effect into account. Therefore the estimation of its importance is still not done.

in chapter 7 the electric potential φ was calculated as the first order perturbation function of the coordinate x but the focusing of ions is caused by the z-dependence of H_{i1}. Therefore the perturbation of φ has to be calculated up to the second order contribution.

Densities and electric potential are represented as

$$n_\alpha = n_{e0}\left(\rho_\alpha(\xi) + \rho_{\alpha 2}(\xi)\cos(\pi z/L)\right), \quad \varphi = \varphi_a\left(u(\xi) + u_2(\xi)\cos(\pi z/L)\right) \tag{84}$$

with the constant dimensionless electron density $\rho_e = 1$ and the functions u , ρ_i being the results of the one dimensional analysis of chapter 5.2. According to Eq. (23) for small values of ε_i and for the ion flux given by Eq. (39) at the equality $\iota = 1/2$ it is obtained $\rho_i = (1\text{-}u)^{-1/2}/2$. The function u is given by Eq. (49).

Substituting Eq. (84) into Eq. (4) and using Eq. (47) for the parameter ε_D the equation for the function u_2 is obtained as a zero coefficient at the function $\cos(\pi z/L)$:

$$\frac{d^2u_2}{d\xi^2} - \varepsilon_z^2 u_2 = \tfrac{1}{2}\pi^2\left(\rho_{e2} - \rho_{i2}\right), \qquad u_2(0) = u_2(1) = 0 \tag{85}$$

with the dimensionless parameter $\varepsilon_z = \pi l/L$. The condition at the boundary $\xi = 1$ in Eq. (85) is valid due to the equality $\eta(1) = 0$. This fact is proved similarly to Eq. (78) by the shift of the boundary condition from $\sigma = 0$ resulting in $u_2(1) = \eta(1)a_1/l$. The functions η and σ are given by Eqs. (50) and (70).

In order to calculate the electron density correction ρ_{e2} the Boltzmann distribution function f_e along the magnetic surface $A_y = -(c/e)p_y$ = constant with the potential A_y given by Eq. (77) is obtained according to Eq. (17) in the linear approximation for the exponent as

$$f_e\left(x, z, H, p_y\right) = f_{e0}|_{z=0}\left(1 + \left(e/T_{em}\right)\left(\varphi(x,z) - \varphi(x_c,0)\right)\right) \tag{86}$$

The Maxwellian function $f_{e0}|_{z=0}$ is defined by Eq. (15) at constant central density $n_{em} = n_{e0}$ and temperature T_{em}. The Maxwellian function doesn't dependent on the coordinate x. In Eq. (86) the coordinate x_c at the plane $z = 0$ belongs to the magnetic surface that crosses the point (x,z), thus according to Eq. (77) the following relation between the coordinates x and x_c is valid:

$$w(x_c/l) + l^{-1}a(x_c) = w(x/l) + l^{-1}a(x)\cos(\pi z/L)$$

Neglecting the difference between the coordinates x and x_c in the small amplitude a and using the function $w(x) = 1 - x/l$ in accordance with Eq. (52), the expression for x_c is obtained as:

$$x_c = x + a(x)\left(1 - \cos(\pi z/L)\right)$$

As a result the potential dependence on x and z is obtained in the linear approximation as:

$$\varphi(x_c,0) = \varphi_a\left(u - \eta\frac{a}{l}\left(1 - \cos(\pi z/L)\right)\right)$$

Hence from Eq. (86) the electron density n_e is obtained as

$$n_e = n_{e0}\left(1 + \varepsilon_T^{-1}\eta\frac{a}{l} + \varepsilon_T^{-1}\left(u_2 - \eta\frac{a}{l}\right)\cos(\pi z/L)\right)$$

with the dimensionless parameter $\varepsilon_T = T_{em}/e\varphi_a$. In these expressions for the density and the potential there are small terms which don't depend on the coordinate z. Such terms are not important for focusing and thus are neglected. As a result the correction ρ_{e2} is obtained as

$$\rho_{e2} = \varepsilon_T^{-1}\left(u_2 - \eta\frac{a}{l}\right) \tag{87}$$

For the calculation of ρ_{i2} only the dependence of the electrical term on z in Eq. (83) has to be taken into account. This part has to be used for calculation of the correction f_{i1} on the base of Eq. (63). Thus the sufficient part of f_{i1} is given as:

$$f_{i1} = e\varphi_a\left[\frac{\partial f_{i0}}{\partial H}u_2\cos(\pi z/L) - \frac{\pi}{L}\frac{\partial f_{i0}}{\partial p_z}\int_0^t u_2(\xi(t'))dt'\sin(\pi z/L)\right] \tag{88}$$

Since the second term in the RHS of Eq. (88) is an odd function of the p_z, there is no contribution of this term to the ion density integral $n_{i1}=n_{e0}\rho_{i2}$ of Eq. (65). The calculation of Eq. (65) for the small parameter ε_i using Eq. (39) with $\iota = 1/2$ results in an expression for ρ_{i2}:

$$\rho_{i2} = \frac{u_2}{4(1-u)^{3/2}} \tag{89}$$

After substituting Eqs. (87), (89) and (80), Eq. (85) can be written as:

$$\frac{d^2u_2}{d\xi^2} - \left(\varepsilon_z^2 + \frac{\pi^2}{2\varepsilon_T} - \frac{\pi^2}{8(1-u)^{3/2}}\right)u_2 = -\frac{\pi^2}{2\varepsilon_T}\eta\frac{a_1}{l}\frac{\mathrm{sh}(\varepsilon_z\xi)}{\mathrm{sh}\varepsilon_z},\quad u_2(0) = u_2(1) = 0 \tag{90}$$

In order to simplify the further analysis a small value is assumed for the parameter ε_T (the case of relatively cold electrons in the gap when the inequality $T_{em} << e\varphi_a$ is valid). Due to this assumption only the terms containing large parameter $G = \pi^2/2\varepsilon_T$ are saved in Eq. (90). The simplified equation is becoming the algebraic expression for the function u_2:

$$u_2 = \eta\frac{a_1}{l}\frac{\mathrm{sh}(\varepsilon_z\xi)}{\mathrm{sh}\varepsilon_z} \tag{91}$$

This solution is valid in the main volume of the gap except at the rather thin electrostatic sheaths. These sheaths there are formed to satisfy the boundary conditions. A sheath near the virtual cathode forms to satisfy the condition $u_2(1) = 0$. To achieve this the terms $d^2u_2/d\xi^2$ and Gu_2 of Eq. (90) are becoming comparable near the virtual cathode. The thickness l_c of the

layer is estimated as $l_c = l/G^{1/2} << 1$ with $G = \pi^2/2\varepsilon_T$. The sheath near the anode of the thickness $l_a \sim l_c$ concerns the large value of the term $\pi^2/[8(1-u)^{3/2}]u_2$ at $u \approx 1$[7]. A small influence of the sheath is neglected below.

The ion flux z-component j_{iz2} of Eq. (66) is integrated taking into account only a contribution from the odd part of the function f_{i1} with respect to the momentum component p_z because the contributions from the even part of this function and from the even term containing the Hamilton function correction H_{i1} are equal to zero due to the factor p_z under the integral. Thus the relation of the z- to the x-components of the ion flux at the virtual cathode is obtained as

$$\left(j_{iz2}/j_{ix1}\right)_{x=l} = \frac{\pi^2 z a_1}{L^2}\int_0^1 \frac{\eta(\xi)\mathrm{sh}(\varepsilon_z\xi)}{\mathrm{sh}\varepsilon_z\sqrt{1-u(\xi)}}d\xi \tag{92}$$

The integral in Eq. (76) was calculated for $\varepsilon_z << 1$ ("shallow gap"), $\varepsilon_z >> 1$ ("deep gap") and $\varepsilon_z = 1$. At $\varepsilon_z << 1$ the integral is equal to $(2\pi)^{-1}$. At $\varepsilon_z >> 1$ only a small interval of the thickness $l_z = L/\pi$ near the virtual cathode is important for the calculation. Assuming that the parameter ε_T is small enough for the neglection of the sheath at the virtual cathode ($l_z >> l_c$) the integral is calculated as $\pi/[4(\varepsilon_z)^2]$. For the intermediate case $\varepsilon_z = 1$ numerical integration results in the approximate value 1/7.

Finally using Eqs (67), (68), (82) and (92) the focal distance F is obtained as

$$F = \varepsilon_a^{-2}\tfrac{16}{3}\left(L/\pi^3\right)\left(\mathrm{cth}\varepsilon_z + \mathrm{cth}(\pi h/L)\right)\times\begin{bmatrix} 2\pi & \text{for } \varepsilon_z << 1 \\ 7 & \text{for } \varepsilon_z = 1 \\ 4\varepsilon_z^2/\pi & \text{for } \varepsilon_z >> 1 \end{bmatrix} \tag{93}$$

For example, the high voltage proton diode has the following parameters: $l = h = 1$ cm, $L = 3.14$ cm, the applied magnetic field A_a/l is 3 T, the voltage φ_a is 5 MV. Then the values of the dimensionless parameters are equal to $\varepsilon_z = 1$ and $\varepsilon_a = 5/9$. The focal distance is obtained as $F \approx 32.5$ cm. There is a minimum of the function $F(\varepsilon_z)$ at fixed values of the parameters ε_a and h/l. For $h = l = 1$ cm and $\varepsilon_a = 5/9$, F reaches the minimum value $F_{min} = 24$ cm at $\varepsilon_z = 1.3$ ($L = 2.4$ cm). A further increase of the potential moves the focal point towards the electrodes. The perturbation model can't be applied anymore.

The parameter ε_a can be expressed as $\varepsilon_a = \upsilon_D/c$ with $\upsilon_D = cE_x/B_z \approx \varphi_a/A_a$ the characteristic electron drift velocity in the gap. In the limit $\varepsilon_a \to 1$ the drift velocity in the diode should approach the velocity of light. In this case at small electron temperature T_0 the Buneman instability should develop increasing T_0 self consistently.

---

[7] An analysis of the anode layer at $x<l_a$ the details of which are omitted here implies this term as important as the RHS of Eq. (90). According to the analysis the only possible solution satisfying the condition $u_2(0) = 0$ is obtained as $u_2 \approx -(72/585)(3\pi/5)^{1/3}G\xi^{10/3}(a_1/l)$. Comparing this result with Eq. (91) at $\xi = G^{-1/2}$ and $\varepsilon_z < 1$ it is checked that both solutions are proportional to $G^{-2/3}$ but they have different signs, the solution Eq. (91) is absolutely larger by the factor 585/72. Thus the function u_2 changes the sign in the sheath. This circumstance doesn't destroy monotonic behavior of the whole electric potential.

8. CONCLUSION

At non-relativistic ion velocities the effect of the magnetic self-focusing is of the order of $(V_i/c)^2$ with V_i the velocity of accelerated ions at the cathode. The effect of self focusing due to the curvature of the virtual cathode is of the order of $(\varphi_a/A_a)^2$. At $\varphi_a < A_a$ the focus distance F is significantly larger than the characteristic dimensions of the diode. To obtain the dependence of F on the higher voltage φ_a (at F comparable with the diode electrode sizes l, h and L) either a higher order perturbation analysis with the small parameter $(\varphi_a/A_a)^2$ or a direct numerical calculation are necessary. For available installations φ_a/A_a doesn't exceed the value of 0.5 . Therefore for the development of a comprehensive model for an analysis of turbulent processes it is sufficient to use a plane 1 dim approach (in the simplest case the solution of chapter 5.2) as an adequate initial approximation neglecting the effects of self focusing as long as the electric potential is not extremely high.

9. REFERENCES

1. M. Desjarlais, Theory of applied-B ion diodes, Phys. Fluids B, **1**, 1709, 1989.
2. A.V. Gordeev, A.V. Grechikha, New model for electron screening in an ion diode in an external magnetic field, JETP Lett., **61**, 196, 1996.
3. M. Boger, E. Halter, M. Krauß, C.-D. Munz, R. Schneider, E. Stein, U. Voß, T. Westermann, The Karlsruhe Diode Simulation Program System KADI2D, FZK, Annual report FZKA 5840, 69, 1995.
4. A. Grechikha, Electron sheath collapse in an applied-B ion diode, FZK, Annual report FZKA 5840, 61, 1995.
5. J.P. Quintenz, D. B. Seidel, M.L. Kiefer, T.D. Pointon, R.S. Coats, S.E. Rosenthal, T.A. Mehlhorn, M.P. Desjarlais, N.A. Krall, Simulation codes for light-ion diode modeling, Laser and Particle Beams, **12**, 283, 1994.
6. T.D. Pointon, M.P. Desjarlais, Three-dimensional particle-in-cell simulations of applied-B ion diodes on the particle beam fusion accelerator II, J. Appl. Phys., **80**, 2079, 1996.
7. V.P. Pastukhov, Anomalous electron transport in the transition layer of an electrostatically plugged magnetic mirror, Sov. J. Plasma Phys. **6**, 549, 1980.
8. A.A. Galeev, R.Z. Sagdeev, In: Reviews of Plasma Physics, 7, Consultants Bureau, New York, 1974.
9. L.D.Landau, E.M.Lifshitz, Mechanics. Pergamon Press, 1959.
10. L.D.Landau, E.M.Lifshitz, The classical theory of fields. Pergamon Press, 1959.

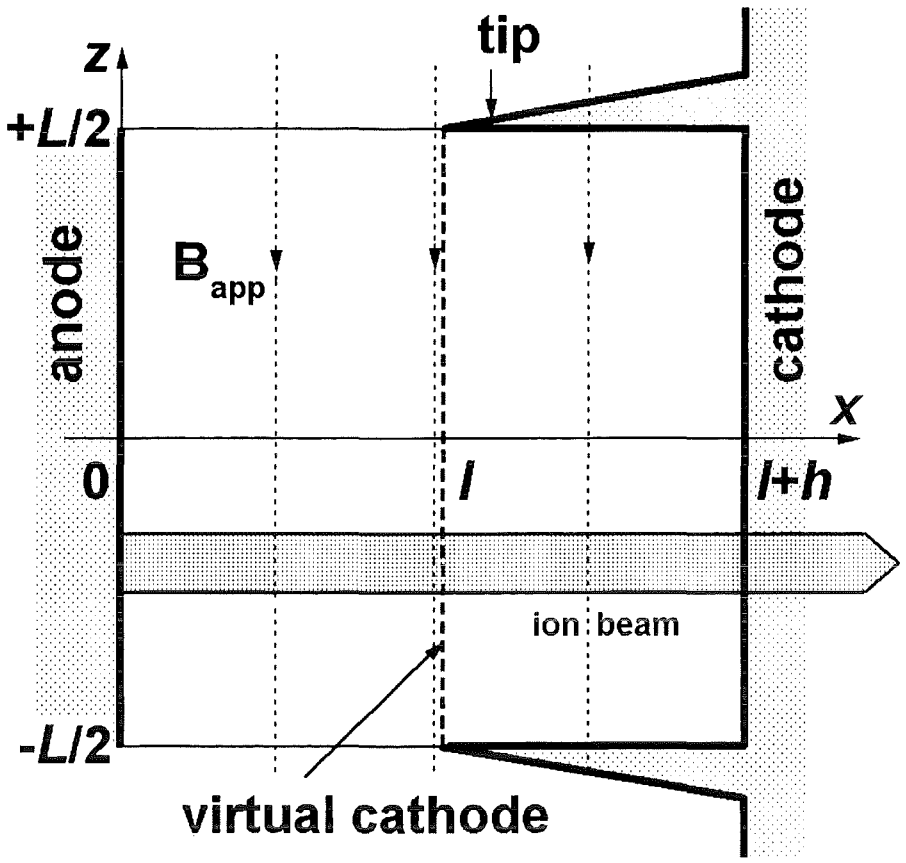

Fig. 1 Principal scheme of a diode

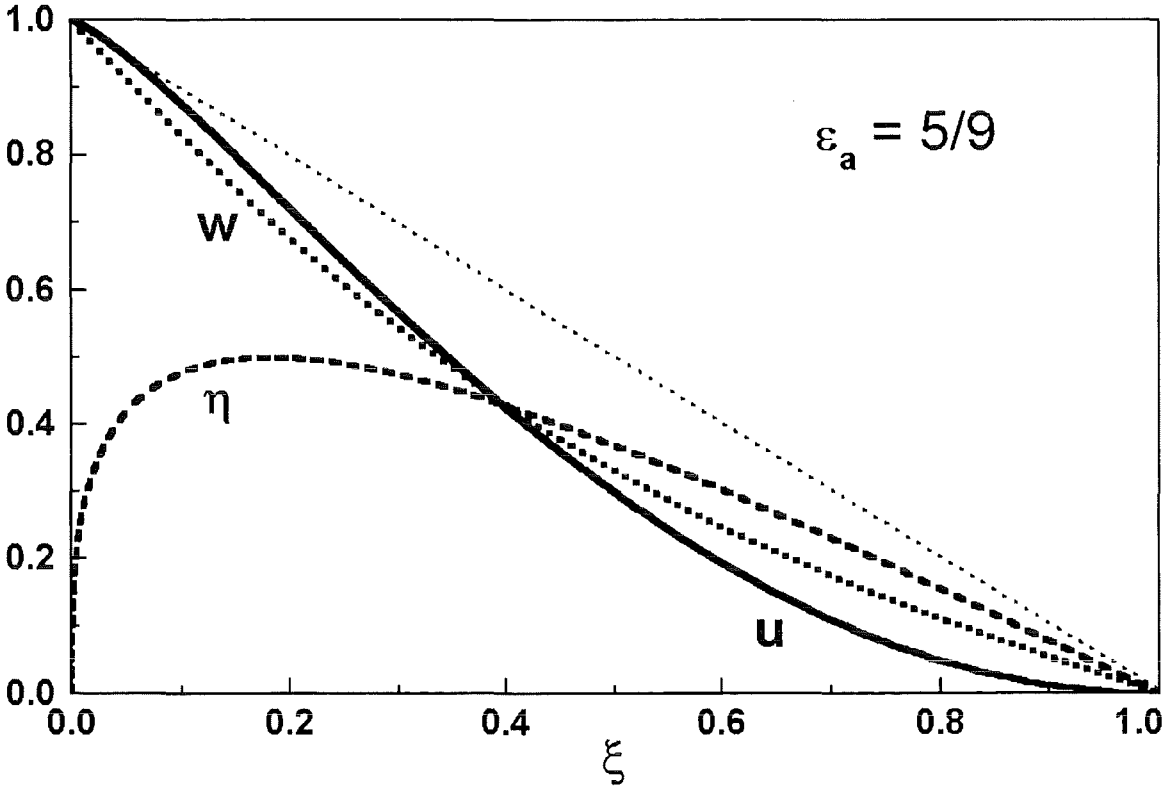

Fig. 2 Dependence of dimensionless functions electric (u) and magnetic (w) potentials as well as electric field strength η on dimensionless coordinate ξ

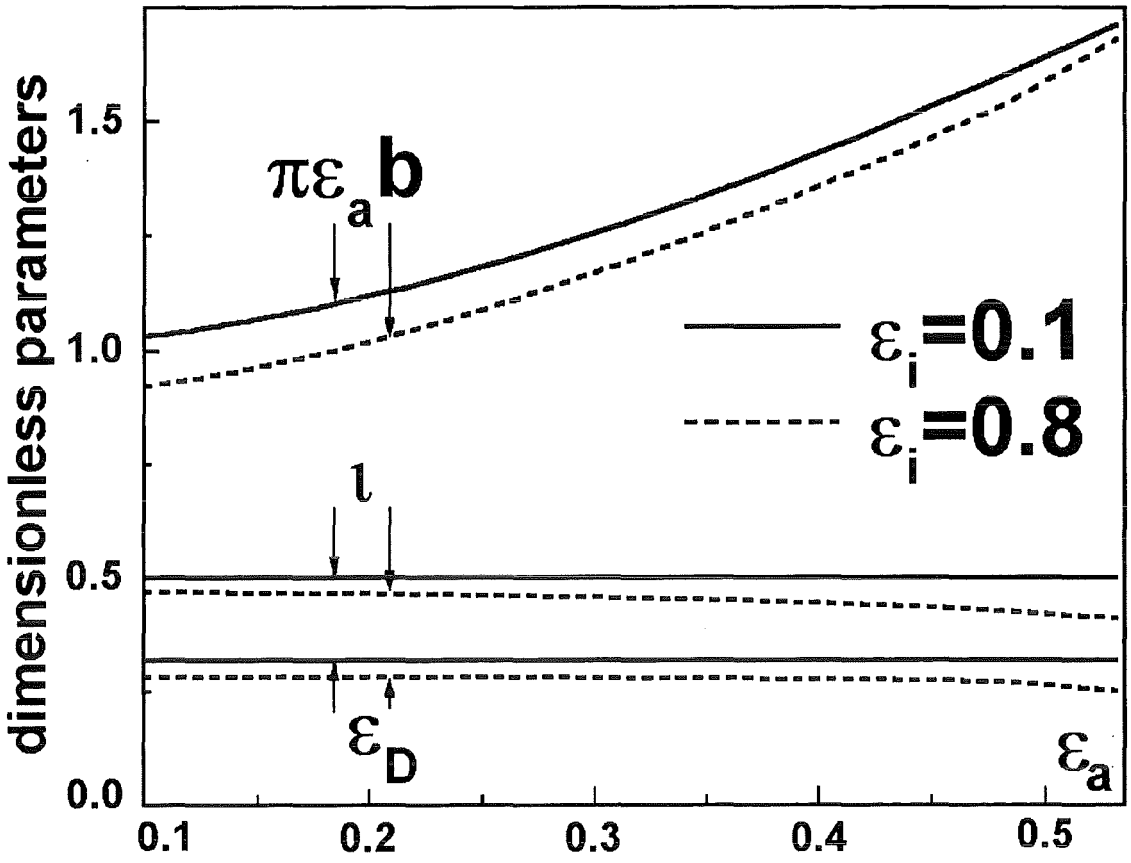

Fig. 3 Dependence of the dimensionless parameters anode magnetic field strength(b), ion flux(l) and Debye length (ε_D) on dimensionless anode electric potential ε_a

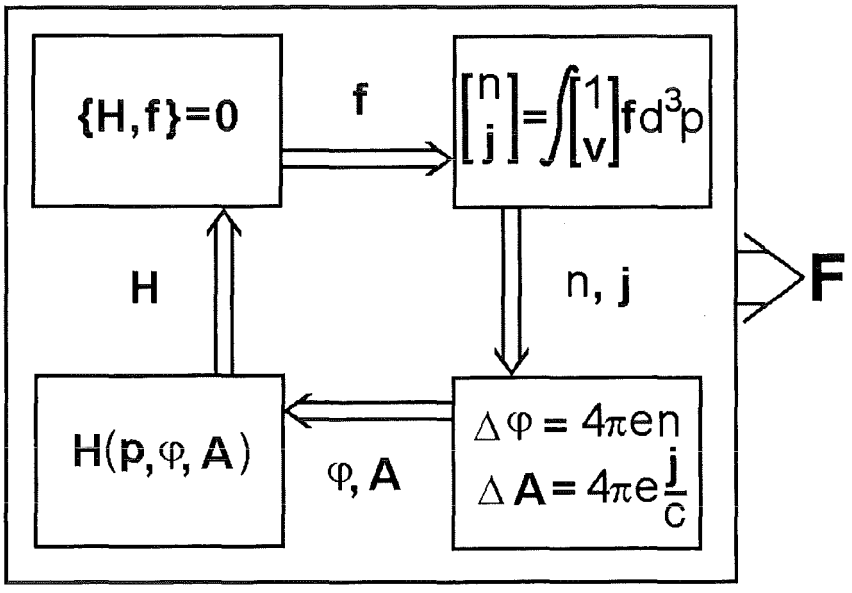

Fig. 4 Scheme of consistent calculation of the focal length

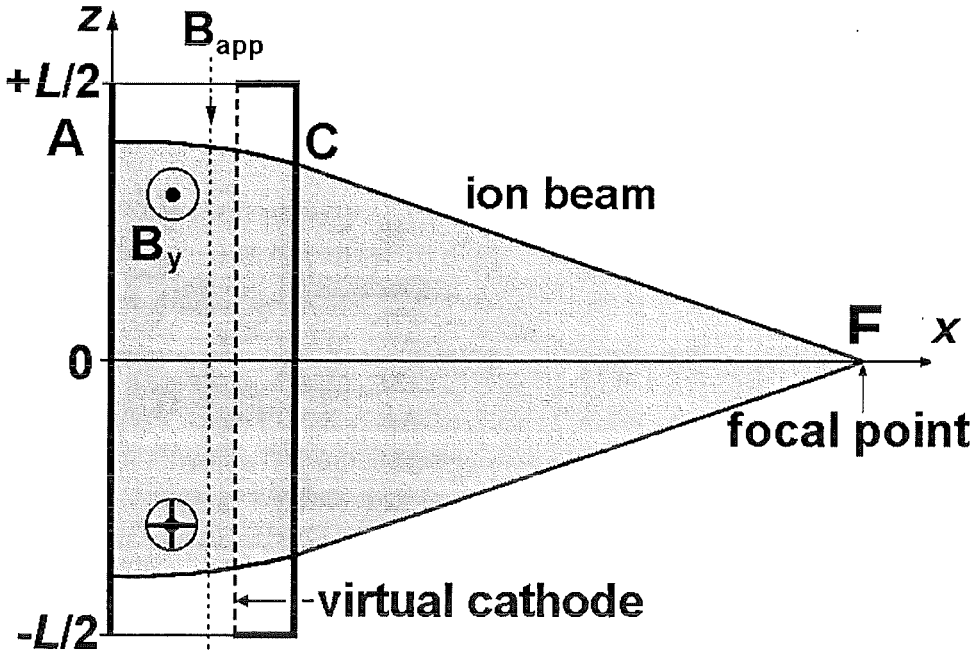

Fig. 5 Magnetic self - focusing schematically

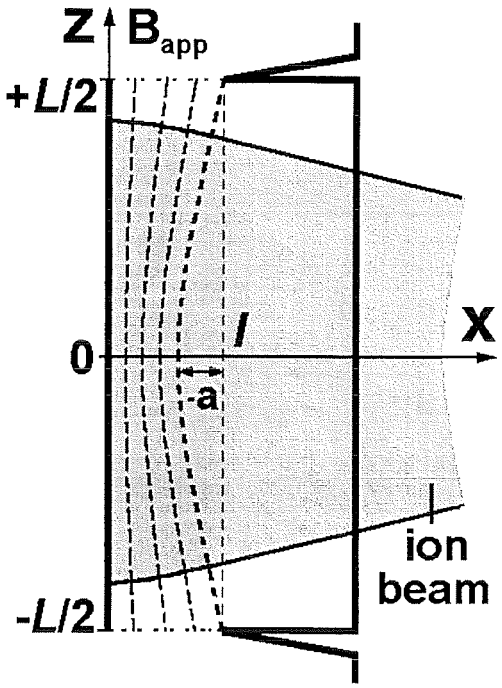

Fig. 6 Diamagnetic self focusing schematically